

Received 3 June 2020
Accepted 30 June 2020

Edited by M. Zeller, Purdue University, USA

Keywords: crystal structure; 2-hydroxy-5-methylbenzaldehyde; 2 aminobenzonitrile; Schiff base.

CCDC reference: 2013269

Supporting information: this article has supporting information at journals.iucr.org/e

Crystal structure, Hirshfeld surface analysis and DFT studies of 2-[(2-hydroxy-5-methylbenzylidene)amino]benzonitrile

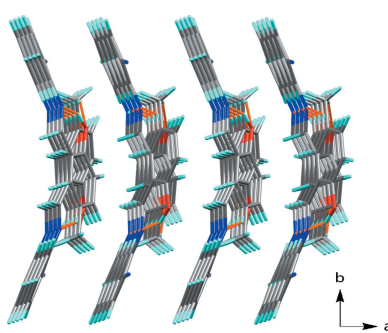
Md. Serajul Haque Faizi,^a Emine Berrin Cinar,^b Alev Sema Aydin,^c Erbil Agar,^c Necmi Dege^b and Ashraf Mashrai^{d*}

^aDepartment of Chemistry, Langat Singh College, B.R.A. Bihar University, Muzaffarpur, Bihar-842001, India, ^bOndokuz Mayis University, Faculty of Arts and Sciences, Department of Physics, Samsun, Turkey, ^cOndokuz Mayis University, Faculty of Arts and Sciences, Department of Chemistry, Samsun, Turkey, and ^dDepartment of Pharmacy, University of Science and Technology, Ibb Branch, Ibb, Yemen. *Correspondence e-mail: ashraf.yemen7@gmail.com

The title compound, $C_{15}H_{12}N_2O$, was synthesized by condensation reaction of 2-hydroxy-5-methylbenzaldehyde and 2-aminobenzonitrile, and crystallizes in the orthorhombic space group $Pbca$. The phenol ring is inclined to the benzonitrile ring by $25.65(3)^\circ$. The configuration about the $C=N$ bond is *E*, stabilized by a strong intramolecular $O-H\cdots N$ hydrogen bond that forms an $S(6)$ ring motif. In the crystal, $C-H\cdots O$ and $C-H\cdots N$ interactions lead to the formation of sheets perpendicular to the a axis. $C-H\cdots \pi$ interactions, forming polymeric chains along the a -axis direction, connect these sheets into a three-dimensional network. A Hirshfeld surface analysis indicates that the most important contributions for the packing arrangement are from $H\cdots H$ and $C\cdots H/H\cdots C$ interactions. The density functional theory (DFT) optimized structure at the B3LYP/6-311 G(d,p) level is compared with the experimentally determined molecular structure and the HOMO–LUMO energy gap is given.

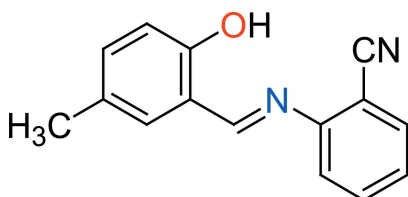
1. Chemical context

Schiff bases containing the azomethine moiety ($-RCH=N-R'$) are prepared by a condensation reaction between amines and reactive carbonyl compounds, such as aldehydes. Schiff bases are employed as catalyst carriers (Grigoras *et al.*, 2001), thermo-stable materials (Vančo *et al.*, 2004), metal–cation complexing agents and in biological systems (Taggi *et al.*, 2002). They also show biological activities such as antibacterial, antifungal, anticancer, antiviral and herbicidal (Desai *et al.*, 2001; Singh & Dash, 1988; Karia & Parsania, 1999; Siddiqui *et al.*, 2006). Schiff bases are also capable of forming stable complexes by coordination to metal ions *via* their nitrogen donor atoms (Ebrahimipour *et al.*, 2012). They are important for their photochromic properties and have applications in various fields such as the measurement and control of radiation intensities in imaging systems and in optical computers, electronics, optoelectronics and photonics (Iwan *et al.*, 2007). *ortho*-Hydroxy Schiff base compounds such as the title compound can display two tautomeric forms, the enol-imine (OH) and keto-amine (NH) forms. Depending on the tautomers, two types of intramolecular hydrogen bonds are generally observed in *ortho*-hydroxy Schiff bases, namely $O-H\cdots N$ in enol-imine and $N-H\cdots O$ in keto-amine tautomers (Tanak *et al.*, 2010). The present work is a part of an ongoing structural study of Schiff bases and their utilization in



OPEN ACCESS

the synthesis of quinoxaline derivatives (Faizi *et al.*, 2018), fluorescence sensors (Faizi *et al.*, 2016; Mukherjee *et al.*, 2018; Kumar *et al.*, 2017; 2018) and non-linear optical properties (Faizi *et al.*, 2020). We report herein the synthesis of the title compound 2-[2-hydroxy-5-methylbenzylidene)amino]benzonitrile (**I**) from 2-hydroxy-5-methylbenzaldehyde and 3-chloro-4-methylaniline, as well as its crystal structure, Hirshfeld surface analysis and DFT computational calculations. The results of calculations by density functional theory (DFT) carried out at the B3LYP/6–311 G(d,p) level are compared with the experimentally determined molecular structure in the solid state.



2. Structural commentary

The molecular structure of the title compound is shown in Fig. 1. The configuration of the $C_8=N_2$ bond of this Schiff base is *E*, stabilized by the intramolecular $O_1-H_1\cdots N_1$ hydrogen bond that forms an *S*(6) ring motif (Fig. 1 and Table 1). This is a relatively common feature in analogous imine-phenol compounds (see *Database survey* section). The $C_{10}-O_1$ bond length [1.3503 (17) Å for X-ray and 1.337 Å for B3LYP] indicates single-bond character, while the imine $C_8=N_2$ bond length [1.2795 (17) Å for X-ray and 1.291 Å for B3LYP] indicates double-bond character. All bond lengths and bond angles are within normal ranges and are comparable with those in related Schiff base compounds (Faizi *et al.*, 2019; Kansiz *et al.*, 2018; Ozeryanskii *et al.*, 2006). The $C_{10}-O_1$ and $C_8=N_2$ bond lengths confirm the enol-imine form of the title compound (Wozniak *et al.*, 1995; Pizzala *et al.*, 2000). The molecule is not planar, with the benzonitrile ring tilted by 25.65 (3)° to the plane of the 5-methylphenol moiety. The imine and 5-methylphenol groups are, however, essentially coplanar, as indicated by the $C_9-C_8-N_2-C_7$ torsion angle

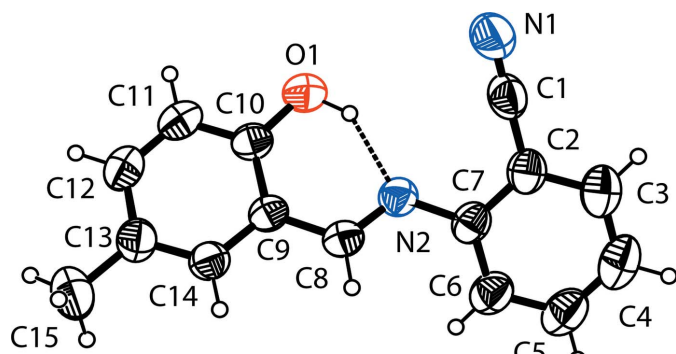


Figure 1

The molecular structure of (**I**) with the atom-numbering scheme. Displacement ellipsoids are drawn at the 40% probability level. The intramolecular $O-H\cdots N$ hydrogen bond (Table 1) is shown as a dashed line.

Table 1
Hydrogen-bond geometry (Å, °).

$Cg1$ is the centroid of the C_9-C_{14} ring.

$D-H\cdots A$	$D-H$	$H\cdots A$	$D\cdots A$	$D-H\cdots A$
$O_1-H_1\cdots N_2$	0.92	1.83	2.6280 (16)	145
$C_4-H_4\cdots N_1^i$	0.93	2.77	3.610 (3)	150
$C_{15}-H_{15A}\cdots O_1^{ii}$	0.96	2.74	3.641 (3)	158
$C_{11}-H_{11}\cdots Cg_1^{iii}$	0.93	2.85	3.654 (16)	146

Symmetry codes: (i) $-x + \frac{1}{2}, -y + 1, z + \frac{1}{2}$; (ii) $x, -y + \frac{1}{2}, z + \frac{1}{2}$; (iii) $x + \frac{1}{2}, -y + \frac{1}{2}, -z + 1$.

of -178.75 (13)° and the $C_1-C_{14}-C_{15}-N_1$ torsion angle [0.31 (3)° for X-ray and 0.44° for B3LYP].

3. Supramolecular features and Hirshfeld surface analysis

The crystal structure of the title compound is consolidated by $C-H\cdots O$ and $C-H\cdots N$ interactions, forming corrugated layers perpendicular to the a axis (Fig. 2, Table 1). The mol-

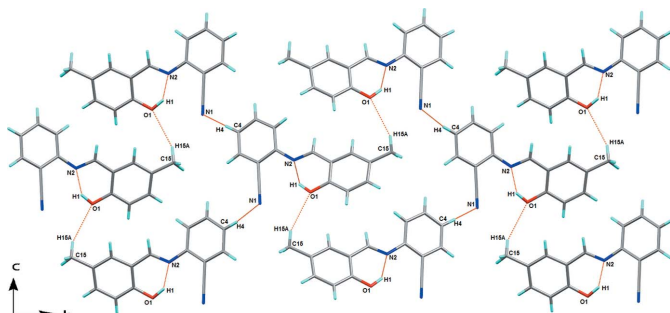


Figure 2

View along the a axis of the unit cell showing the molecular sheets, formed via $C-H\cdots O$ and $C-H\cdots N$ interactions (see Table 1 for details).

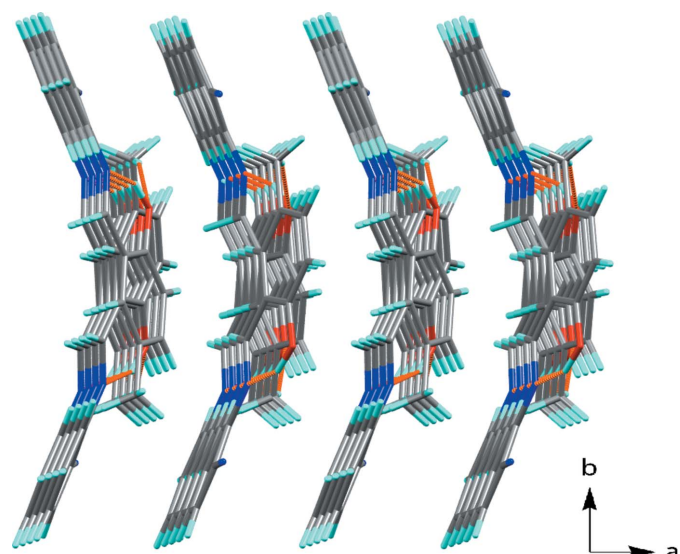


Figure 3

View along the c axis of the unit cell showing the infinite chains, formed via $C-H\cdots\pi$ interactions (see Table 1 for details).

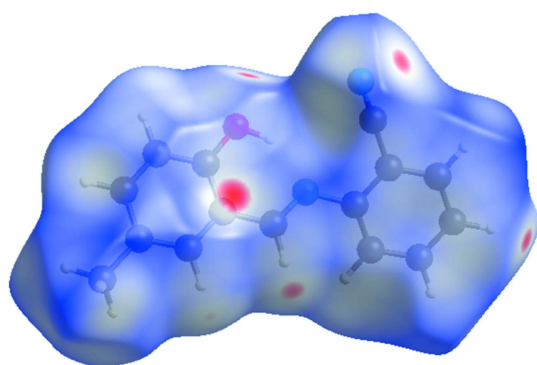


Figure 4
The Hirshfeld surface of compound (I) mapped over d_{norm} .

ecules are also linked through intermolecular C–H \cdots π interactions hydrogen atom H11 and the centroid of the C9–C14 ring at $\frac{1}{2} + x, \frac{1}{2} - y, 1 - z$, which connect molecules along the a -axis direction (Fig. 3). C–H \cdots O, C–H \cdots N and C–H \cdots π interactions combined lead to the formation of a three-dimensional network.

In order to better visualize and analyze the role of weak intermolecular contacts in the crystal, a Hirshfeld surface (HS) analysis (Spackman & Jayatilaka, 2009) was carried out and

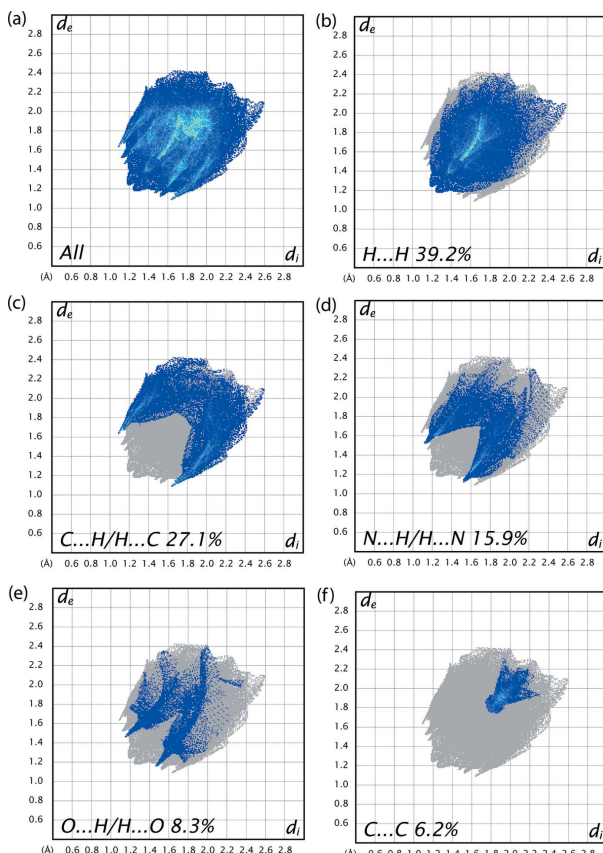


Figure 5
The overall two-dimensional finger print plots for compound (I), and those delineated into: (b) H \cdots H (39.2%), (c) C \cdots H/H \cdots C (27.1%), (d) N \cdots H/H \cdots N (16.0%), (e) O \cdots H/H \cdots O (8.3%) and C \cdots C (6.2%) contacts.

Table 2

Comparison of selected observed (X-ray data) and calculated (DFT) geometric parameters (\AA , $^\circ$).

Parameter	X-ray	B3LYP/6-311G(d,p)
O1–C10	1.3503 (17)	1.3366
N2–C8	1.2795 (17)	1.2909
N2–C7	1.4130 (18)	1.3979
C1–N1	1.138 (2)	1.155
C1–C2	1.436 (3)	1.429
C8–C9	1.4380 (19)	1.4432
N1–C1–C2	179.2 (2)	178.3
C8–N2–C7	121.58 (13)	121.07
N2–C8–C9	122.03 (13)	122.79
C7–N2–C8–C9	−178.75 (13)	−176.57

the associated two-dimensional fingerprint plots (McKinnon *et al.*, 2007) generated using *CrystalExplorer*17.5 (Turner *et al.*, 2017) were analysed. The three-dimensional d_{norm} surface is shown in Fig. 4 with a standard surface resolution and a fixed colour scale of −0.1805 to 1.0413 a.u. The darkest red spots on the Hirshfeld surface indicate contact points with atoms participating in the C–H \cdots π interactions involving C11–H11 and the phenyl substituent (Table 1). As illustrated in Fig. 5*a*, the corresponding fingerprint plots for the compound have characteristic pseudo-symmetric wings along the d_e and d_i diagonal axes. The presence of C–H \cdots π interactions in the crystal is indicated by the pair of characteristic wings in the fingerprint plot delineated into C \cdots H/H \cdots C contacts (Fig. 5*c*, 27.1% contribution to the Hirshfeld surface). As shown in Fig. 5*b*, the most widely scattered points in the fingerprint plot are related to H \cdots H contacts, which make a contribution of 39.2% to the Hirshfeld surface. There are also N \cdots H/H \cdots N (16.0%; Fig. 5*d*), O \cdots H/H \cdots O (8.3%; Fig. 5*e*) and C \cdots C (6.2%; Fig. 5*f*) contacts, with smaller contributions from C \cdots N/N \cdots C (2.6%), C \cdots O/O \cdots C (0.4%) and N \cdots N (0.3%) contacts.

4. DFT calculations

The optimized structure of the title compound in the gas phase was generated theoretically *via* density functional theory (DFT) calculations using the standard B3LYP functional and a 6-311G(d,p) basis-set (Becke, 1993) as implemented in *GAUSSIAN09* (Frisch *et al.*, 2009). The theoretical and experimental results are in good agreement (Table 2). The C8=N2 bond length is 1.2795 (17) \AA for X-ray and 1.291 \AA for B3LYP and the C10–O1 bond length is 1.3503 (17) \AA for X-ray and 1.367 \AA for B3LYP.

The highest-occupied molecular orbital (HOMO) and the lowest-unoccupied molecular orbital (LUMO) are very important parameters for quantum chemistry. Many electronic, optical and chemical reactivity properties of compounds can be predicted from frontier molecular orbitals (Tanak, 2019). A molecule with a small HOMO–LUMO bandgap is more polarizable than one with a large gap and is considered a soft molecule because of its high polarizability, while molecules with a large bandgap are considered to be

'hard molecules'. To better understand the nature of the title compound, the electron affinity ($A = -E_{\text{HOMO}}$), the ionization potential ($I = -E_{\text{LUMO}}$), HOMO–LUMO energy gap (ΔE), the chemical hardness (η) and softness (S) of the title compound were predicted based on the E_{HOMO} and E_{LUMO} energies (Tanak, 2019). For the title compound, $I = 6.146$ eV, $A = 2.223$ eV, $\Delta E = 3.923$ eV, $\eta = 1.961$ eV and $S = 0.311$ eV. Based on the relatively large ΔE and η values, the title compound can be classified as a hard molecule.

The electron distribution of the HOMO-1, HOMO, LUMO and the LUMO+1 energy levels are shown in Fig. 6. The DFT study shows that the HOMO and LUMO are localized in the plane extending from the whole 2-hydroxy-5-methyl-benzaldehyde ring to the 2 aminobenzonitrile unit. The HOMO, HOMO-1 and LUMO orbitals are delocalized over the π systems of the two aromatic rings and connected by the Schiff

base bridge. HOMO and HOMO-1 can be said to be π -bonding with respect to the C=N imine bond, while the LUMO orbital has imine π^* antibonding character. The LUMO+1 orbital on the other hand is localized only on the aminobenzonitrile ring and the C atom of the Schiff base. With respect to the imine π -bond it is mostly non-bonding. From the frontier orbital analysis, it can be concluded that a HOMO-to-LUMO excitation of (I) would be a $\pi-\pi^*$ transition that would weaken the imine bond and drive the production of an excited-state keto–amine tautomer from the enol–imine ground state observed in the solid state. The calculated bandgap of (I) is 3.923 eV, which is similar to that reported for other Schiff base materials, such as for example (*E*)-2-[(3-chlorophenyl)imino]methyl]-6-methylphenol (energy gap = 4.069 eV; Faizi *et al.*, 2019) and (*E*)-2-[(2-hydroxy-5-methoxybenzylidene)amino]benzonitrile (energy gap = 3.520 eV; Saracoğlu *et al.*, 2020).

5. Database survey

A search of the Cambridge Structural Database (CSD, version 5.39, update of November 2019; Groom *et al.*, 2016) gave 14 hits for a 2-[(2-hydroxy-5-methylphenyl)methylidene]amino]benzonitrile moiety. The eight most closely related compounds are (*E*)-2-[(5-bromo-2-hydroxybenzylidene)amino]benzonitrile (FOWXOF; Zhou *et al.*, 2009a), 5-chloro-2-(2-hydroxybenzylideneamino)benzonitrile (GEJGAE; Cheng *et al.*, 2006), 2-[(2-hydroxy-5-methoxyphenyl)methylidene]amino]benzonitrile (GOGYUZ; Faizi *et al.*, 2019), *trans*-2-(2-hydroxybenzylideneamino)benzonitrile (LOCBOV; Xia *et al.*, 2008), 2-[(2-hydroxy-6-methoxybenzylidene)amino]benzonitrile (LOVDUX; Demircioğlu *et al.*, 2015), (*E*)-2-(2,4-dihydroxybenzylideneamino)benzonitrile (MOZPAT; Liu, 2009), (*E*)-2-(4-diethylamino-2-hydroxybenzylideneamino)benzonitrile (PUJDOO; Wang *et al.*, 2010) and (*E*)-2-[(3,5-di-*tert*-butyl-2-hydroxybenzylidene)amino]benzonitrile (YOVBHU; Zhou *et al.*, 2009b). All of these compounds are enol–imine tautomers, feature an *E* imine configuration and have the same common strong intramolecular O–H…N hydrogen-bonding interaction that stabilizes the molecular conformation and forms an *S*(6) ring motif. The dihedral angles between the aromatic rings are generally smaller than the value of 25.65 (3) $^\circ$ observed for the title compound, with angles between 1.09 (4) $^\circ$ (for FOWXOF and GEJGAE) and 13.84 (13) $^\circ$ (for PUJDOO). Only YOVBHU features angles similar to those of (I), with dihedral angles of 21.74 (5), 27.59 (5) and 27.87 (5) $^\circ$ for the three independent molecules in its structure. Steric crowding within each molecule seem to be no issue for the eight structures analysed, and the varying torsion angles might be the result of subtle effects from crystal packing forces.

6. Synthesis and crystallization

The title compound was prepared by combining solutions of 2-hydroxy-5-methyl-benzaldehyde (38.0 mg, 0.25 mmol) in ethanol (15 ml) and 2-aminobenzonitrile (33.0 mg, 0.25 mmol)

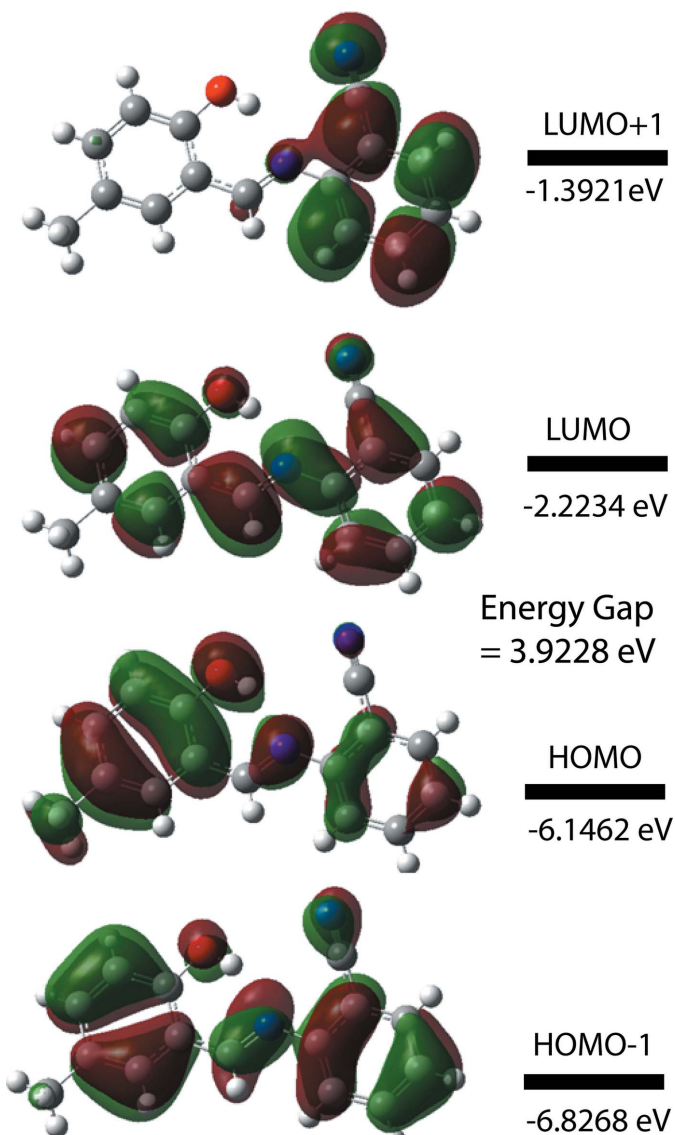


Figure 6

Electron distribution of the HOMO-1, HOMO, LUMO and the LUMO+1 energy levels for the title compound.

in ethanol (15 ml) and stirring the mixture for 5 h under reflux (yield 60%, m.p. 412–414 K). Single crystals of the title compound suitable for X-ray analysis were obtained by slow evaporation of an ethanol solution.

7. Refinement

Crystal data, data collection and structure refinement details are summarized in Table 3. C-bound H atoms were positioned geometrically and refined using a riding model, with C—H = 0.93–0.97 Å and $U_{\text{iso}}(\text{H}) = 1.2\text{--}1.5U_{\text{eq}}(\text{C})$. The position of the H1 atom was obtained from a difference map; it was placed in a calculated position with a fixed C—O—H angle, but the O—H distance and the torsion angle were allowed to freely refine.

Funding information

This study was supported by Ondokuz Mayıs University under project No. PYOFEN.1906.19.001. Funding for this research was provided by a Startup Project, University Grants Commission, India.

References

Table 3 Experimental details.	
Crystal data	
Chemical formula	C ₁₅ H ₁₂ N ₂ O
M_r	236.27
Crystal system, space group	Orthorhombic, Pbc _a
Temperature (K)	296
a, b, c (Å)	7.8139 (3), 27.047 (1), 11.7683 (5)
V (Å ³)	2487.14 (17)
Z	8
Radiation type	Mo $\text{K}\alpha$
μ (mm ⁻¹)	0.08
Crystal size (mm)	0.73 × 0.42 × 0.24
Data collection	
Diffractometer	Stoe IPDS 2
Absorption correction	Integration (X-RED32; Stoe & Cie, 2002)
T_{\min}, T_{\max}	0.951, 0.989
No. of measured, independent and observed [$I > 2\sigma(I)$] reflections	15314, 2270, 1552
R_{int}	0.040
(sin θ/λ) _{max} (Å ⁻¹)	0.602
Refinement	
$R[F^2 > 2\sigma(F^2)], wR(F^2), S$	0.038, 0.103, 1.04
No. of reflections	2270
No. of parameters	167
H-atom treatment	H atoms treated by a mixture of independent and constrained refinement
$\Delta\rho_{\text{max}}, \Delta\rho_{\text{min}}$ (e Å ⁻³)	0.10, -0.09
Computer programs: X-AREA and X-RED32 (Stoe & Cie, 2002), SHELXT2018/3 (Sheldrick, 2015a), SHELXL2018/3 (Sheldrick, 2015b), OLEX2 (Dolomanov <i>et al.</i> , 2009), Mercury (Macrae <i>et al.</i> , 2020), WinGX (Farrugia, 2012), PLATON (Spek, 2020) and publCIF (Westrip, 2010).	
Groom, C. R., Bruno, I. J., Lightfoot, M. P. & Ward, S. C. (2016). <i>Acta Cryst. B</i> 72 , 171–179.	
Iwan, A., Kaczmarszyk, B., Janeczek, H., Sek, D. & Ostrowski, S. (2007). <i>Spectrochim. Acta A Mol. Biomol. Spectrosc.</i> 66 , 1030–1041.	
Kansiz, S., Macit, M., Dege, N. & Pavlenko, V. A. (2018). <i>Acta Cryst. E</i> 74 , 1887–1890.	
Karia, F. D. & Parsania, P. H. (1999). <i>Asian J. Chem.</i> 11 , 991–995.	
Kumar, M., Kumar, A., Faizi, M. S. H., Kumar, S., Singh, M. K., Sahu, S. K., Kishor, S. & John, R. P. (2018). <i>Sens. Actuators B Chem.</i> 260 , 888–899.	
Kumar, S., Hansda, A., Chandra, A., Kumar, A., Kumar, M., Sithambaresan, M., Faizi, M. S. H., Kumar, V. & John, R. P. (2017). <i>Polyhedron</i> , 134 , 11–21.	
Liu, T. (2009). <i>Acta Cryst. E</i> 65 , o1502.	
Macrae, C. F., Sovago, I., Cottrell, S. J., Galek, P. T. A., McCabe, P., Pidcock, E., Platings, M., Shields, G. P., Stevens, J. S., Towler, M. & Wood, P. A. (2020). <i>J. Appl. Cryst.</i> 53 , 226–235.	
McKinnon, J. J., Jayatilaka, D. & Spackman, M. A. (2007). <i>Chem. Commun.</i> pp. 3814–3816.	
Mukherjee, P., Das, A., Faizi, M. S. H. & Sen, P. (2018). <i>Chemistry Select</i> , 3 , 3787–3796.	
Ozeryanskii, V. A., Pozharskii, A. F., Schilf, W., Kamiński, B., Sawka-Dobrowolska, W., Sobczyk, L. & Grech, E. (2006). <i>Eur. J. Org. Chem.</i> pp. 782–790.	
Pizzala, H., Carles, M., Stone, W. E. E. & Thevand, A. (2000). <i>J. Chem. Soc. Perkin Trans. 2</i> , pp. 935–939.	
Saraçoglu, H., Doğan, O. E., Ağar, T., Dege, N. & Iskenderov, T. S. (2020). <i>Acta Cryst. E</i> 76 , 141–144.	
Sheldrick, G. M. (2015a). <i>Acta Cryst. A</i> 71 , 3–8.	
Sheldrick, G. M. (2015b). <i>Acta Cryst. C</i> 71 , 3–8.	
Siddiqui, J. I., Iqbal, A., Ahmad, S. & Weaver, W. (2006). <i>Molecules</i> , 11 , 206–211.	

- Singh, W. M. & Dash, B. C. (1988). *Pesticides*, **22**, 33–37.
- Spackman, M. A. & Jayatilaka, D. (2009). *CrystEngComm*, **11**, 19–32.
- Spek, A. L. (2020). *Acta Cryst. E* **76**, 1–11.
- Stoe & Cie (2002). *X-AREA* and *X-RED32*. Stoe & Cie GmbH, Darmstadt, Germany.
- Taggi, A. E., Hafez, A. M., Wack, H., Young, B., Ferraris, D. & Lectka, T. (2002). *J. Am. Chem. Soc.* **124**, 6626–6635.
- Tanak, H. (2019). *ChemistrySelect* **4**, 10876–10883.
- Tanak, H., Ağar, A. & Yavuz, M. (2010). *J. Mol. Model.* **16**, 577–587.
- Turner, M. J., McKinnon, J. J., Wolff, S. K., Grimwood, D. J., Spackman, P. R., Jayatilaka, D. & Spackman, M. A. (2017). *CrystalExplorer17.5*. The University of Western Australia.
- Vančo, J., Švajlenová, O., Račanská, E. J., Muselík, J. & Valentová, J. (2004). *J. Trace Elem. Med. Biol.* **18**, 155–161.
- Wang, X.-C., Xu, H. & Qian, K. (2010). *Acta Cryst. E* **66**, o528.
- Westrip, S. P. (2010). *J. Appl. Cryst.* **43**, 920–925.
- Wozniak, K., He, H., Klinowski, J., Jones, W., Dziembowska, T. & Grech, E. (1995). *J. Chem. Soc. Faraday Trans.* **91**, 7–85.
- Xia, R., Xu, H.-J. & Gong, X.-X. (2008). *Acta Cryst. E* **64**, o1047–o1047.
- Zhou, J.-C., Li, N.-X., Zhang, C.-M. & Zhang, Z.-Y. (2009a). *Acta Cryst. E* **65**, o1416.
- Zhou, J.-C., Li, N.-X., Zhang, C.-M. & Zhang, Z.-Y. (2009b). *Acta Cryst. E* **65**, o1949.

supporting information

Acta Cryst. (2020). E76, 1195-1200 [https://doi.org/10.1107/S2056989020008907]

Crystal structure, Hirshfeld surface analysis and DFT studies of 2-[(2-hydroxy-5-methylbenzylidene)amino]benzonitrile

Md. Serajul Haque Faizi, Emine Berrin Cinar, Alev Sema Aydin, Erbil Agar, Necmi Dege and Ashraf Mashrai

Computing details

Data collection: *X-AREA* (Stoe & Cie, 2002); cell refinement: *X-AREA* (Stoe & Cie, 2002); data reduction: *X-RED32* (Stoe & Cie, 2002); program(s) used to solve structure: *SHELXT2018/3* (Sheldrick, 2015a); program(s) used to refine structure: *SHELXL2018/3* (Sheldrick, 2015b); molecular graphics: *OLEX2* (Dolomanov *et al.*, 2009), *Mercury* (Macrae *et al.*, 2020); software used to prepare material for publication: *WinGX* (Farrugia, 2012), *PLATON* (Spek, 2020), *SHELXL2018/3* (Sheldrick, 2015b) and *publCIF* (Westrip, 2010).

2-[(2-Hydroxy-5-methylbenzylidene)amino]benzonitrile

Crystal data

$C_{15}H_{12}N_2O$
 $M_r = 236.27$
Orthorhombic, *Pbca*
 $a = 7.8139 (3)$ Å
 $b = 27.047 (1)$ Å
 $c = 11.7683 (5)$ Å
 $V = 2487.14 (17)$ Å³
 $Z = 8$
 $F(000) = 992$

$D_x = 1.262$ Mg m⁻³
Mo $K\alpha$ radiation, $\lambda = 0.71073$ Å
Cell parameters from 13160 reflections
 $\theta = 1.5\text{--}25.8^\circ$
 $\mu = 0.08$ mm⁻¹
 $T = 296$ K
Prism, colorless
0.73 × 0.42 × 0.24 mm

Data collection

STOE IPDS 2
diffractometer
Radiation source: sealed X-ray tube, 12 x 0.4
mm long-fine focus
Plane graphite monochromator
Detector resolution: 6.67 pixels mm⁻¹
rotation method scans
Absorption correction: integration
(X-RED32; Stoe & Cie, 2002)

$T_{\min} = 0.951$, $T_{\max} = 0.989$
15314 measured reflections
2270 independent reflections
1552 reflections with $I > 2\sigma(I)$
 $R_{\text{int}} = 0.040$
 $\theta_{\max} = 25.3^\circ$, $\theta_{\min} = 1.5^\circ$
 $h = -9 \rightarrow 9$
 $k = -32 \rightarrow 32$
 $l = -14 \rightarrow 14$

Refinement

Refinement on F^2
Least-squares matrix: full
 $R[F^2 > 2\sigma(F^2)] = 0.038$
 $wR(F^2) = 0.103$
 $S = 1.04$
2270 reflections

167 parameters
0 restraints
Primary atom site location: dual
Secondary atom site location: difference Fourier
map

Hydrogen site location: inferred from neighbouring sites

H atoms treated by a mixture of independent and constrained refinement

$$w = 1/[\sigma^2(F_o^2) + (0.0529P)^2 + 0.0539P]$$

where $P = (F_o^2 + 2F_c^2)/3$

$$(\Delta/\sigma)_{\max} < 0.001$$

$$\Delta\rho_{\max} = 0.10 \text{ e } \text{\AA}^{-3}$$

$$\Delta\rho_{\min} = -0.09 \text{ e } \text{\AA}^{-3}$$

Extinction correction: SHELXL-2018/3

(Sheldrick 2018),

$$Fc^* = kFc[1 + 0.001x Fc^2 \lambda^3 / \sin(2\theta)]^{-1/4}$$

Extinction coefficient: 0.0048 (9)

Special details

Geometry. All esds (except the esd in the dihedral angle between two l.s. planes) are estimated using the full covariance matrix. The cell esds are taken into account individually in the estimation of esds in distances, angles and torsion angles; correlations between esds in cell parameters are only used when they are defined by crystal symmetry. An approximate (isotropic) treatment of cell esds is used for estimating esds involving l.s. planes.

Fractional atomic coordinates and isotropic or equivalent isotropic displacement parameters (\AA^2)

	<i>x</i>	<i>y</i>	<i>z</i>	$U_{\text{iso}}^*/U_{\text{eq}}$
C1	0.4510 (2)	0.43624 (6)	0.56936 (18)	0.0817 (5)
C2	0.4377 (2)	0.43849 (6)	0.69096 (14)	0.0740 (4)
C3	0.3751 (3)	0.48102 (6)	0.7420 (2)	0.0926 (5)
H3	0.343203	0.507974	0.697713	0.111*
C4	0.3606 (3)	0.48315 (8)	0.8578 (2)	0.1034 (6)
H4	0.316746	0.511334	0.892460	0.124*
C5	0.4108 (3)	0.44357 (8)	0.92255 (18)	0.0991 (6)
H5	0.401374	0.445315	1.001220	0.119*
C6	0.4752 (2)	0.40119 (6)	0.87308 (15)	0.0836 (5)
H6	0.510544	0.374922	0.918342	0.100*
C7	0.48704 (18)	0.39788 (5)	0.75604 (13)	0.0686 (4)
C8	0.54747 (18)	0.31307 (5)	0.73859 (12)	0.0641 (4)
H8	0.499419	0.308529	0.810127	0.077*
C9	0.61539 (17)	0.27095 (5)	0.67918 (11)	0.0598 (4)
C10	0.69055 (18)	0.27512 (6)	0.57110 (12)	0.0654 (4)
C11	0.7545 (2)	0.23368 (6)	0.51800 (14)	0.0759 (4)
H11	0.805539	0.236438	0.446900	0.091*
C12	0.7430 (2)	0.18837 (7)	0.56968 (15)	0.0800 (5)
H12	0.787489	0.160829	0.532733	0.096*
C13	0.6667 (2)	0.18226 (6)	0.67585 (15)	0.0780 (5)
C14	0.6052 (2)	0.22403 (5)	0.72774 (13)	0.0696 (4)
H14	0.554152	0.220906	0.798775	0.084*
C15	0.6544 (3)	0.13194 (6)	0.7305 (2)	0.1221 (8)
H15A	0.673066	0.134971	0.810847	0.183*
H15B	0.739587	0.110501	0.698457	0.183*
H15C	0.542781	0.118329	0.717044	0.183*
O1	0.70348 (16)	0.31893 (4)	0.51676 (10)	0.0877 (4)
H1	0.654 (3)	0.3432 (6)	0.5601 (13)	0.132*
N1	0.4603 (3)	0.43494 (6)	0.47293 (15)	0.1085 (6)
N2	0.55113 (16)	0.35659 (5)	0.69604 (10)	0.0681 (3)

Atomic displacement parameters (\AA^2)

	U^{11}	U^{22}	U^{33}	U^{12}	U^{13}	U^{23}
C1	0.0981 (12)	0.0574 (9)	0.0896 (13)	0.0001 (8)	-0.0131 (11)	-0.0016 (9)
C2	0.0722 (9)	0.0636 (9)	0.0861 (11)	-0.0043 (7)	-0.0017 (8)	-0.0097 (9)
C3	0.0903 (12)	0.0715 (11)	0.1160 (15)	0.0009 (9)	-0.0017 (11)	-0.0165 (11)
C4	0.1000 (14)	0.0856 (13)	0.1245 (18)	0.0013 (11)	0.0128 (13)	-0.0354 (13)
C5	0.1078 (14)	0.0977 (14)	0.0919 (13)	-0.0108 (12)	0.0155 (11)	-0.0295 (12)
C6	0.0909 (12)	0.0832 (11)	0.0766 (11)	-0.0075 (9)	0.0047 (9)	-0.0145 (9)
C7	0.0653 (9)	0.0666 (9)	0.0738 (10)	-0.0066 (7)	0.0033 (7)	-0.0123 (8)
C8	0.0613 (8)	0.0729 (9)	0.0582 (8)	-0.0055 (7)	0.0024 (7)	-0.0020 (7)
C9	0.0557 (7)	0.0681 (9)	0.0558 (8)	-0.0041 (6)	-0.0009 (6)	-0.0045 (7)
C10	0.0618 (8)	0.0749 (10)	0.0597 (8)	-0.0040 (7)	-0.0004 (7)	-0.0017 (8)
C11	0.0704 (9)	0.0948 (12)	0.0624 (9)	0.0027 (9)	0.0066 (7)	-0.0124 (9)
C12	0.0785 (10)	0.0809 (11)	0.0804 (11)	0.0103 (8)	0.0002 (9)	-0.0180 (9)
C13	0.0823 (11)	0.0691 (10)	0.0827 (11)	0.0009 (8)	0.0020 (9)	-0.0063 (8)
C14	0.0729 (9)	0.0715 (9)	0.0645 (9)	-0.0027 (7)	0.0048 (7)	-0.0020 (8)
C15	0.156 (2)	0.0725 (12)	0.1380 (18)	0.0078 (13)	0.0243 (15)	0.0080 (12)
O1	0.1075 (9)	0.0844 (8)	0.0713 (7)	-0.0015 (7)	0.0194 (6)	0.0055 (6)
N1	0.1567 (16)	0.0760 (10)	0.0927 (12)	0.0039 (9)	-0.0181 (11)	0.0018 (9)
N2	0.0721 (8)	0.0658 (8)	0.0663 (7)	-0.0029 (6)	0.0019 (6)	-0.0029 (6)

Geometric parameters (\AA , $^\circ$)

C1—N1	1.138 (2)	C9—C14	1.3940 (19)
C1—C2	1.436 (3)	C9—C10	1.406 (2)
C2—C3	1.387 (2)	C10—O1	1.3503 (17)
C2—C7	1.393 (2)	C10—C11	1.377 (2)
C3—C4	1.369 (3)	C11—C12	1.371 (2)
C3—H3	0.9300	C11—H11	0.9300
C4—C5	1.371 (3)	C12—C13	1.394 (2)
C4—H4	0.9300	C12—H12	0.9300
C5—C6	1.381 (2)	C13—C14	1.371 (2)
C5—H5	0.9300	C13—C15	1.509 (2)
C6—C7	1.383 (2)	C14—H14	0.9300
C6—H6	0.9300	C15—H15A	0.9600
C7—N2	1.4130 (18)	C15—H15B	0.9600
C8—N2	1.2795 (17)	C15—H15C	0.9600
C8—C9	1.4380 (19)	O1—H1	0.92 (2)
C8—H8	0.9300		
N1—C1—C2	179.2 (2)	C10—C9—C8	122.05 (13)
C3—C2—C7	120.90 (16)	O1—C10—C11	118.18 (14)
C3—C2—C1	119.48 (16)	O1—C10—C9	122.02 (14)
C7—C2—C1	119.62 (14)	C11—C10—C9	119.80 (15)
C4—C3—C2	119.7 (2)	C12—C11—C10	120.16 (15)
C4—C3—H3	120.2	C12—C11—H11	119.9
C2—C3—H3	120.2	C10—C11—H11	119.9

C3—C4—C5	119.78 (19)	C11—C12—C13	122.10 (15)
C3—C4—H4	120.1	C11—C12—H12	119.0
C5—C4—H4	120.1	C13—C12—H12	119.0
C4—C5—C6	121.21 (19)	C14—C13—C12	116.84 (15)
C4—C5—H5	119.4	C14—C13—C15	122.08 (17)
C6—C5—H5	119.4	C12—C13—C15	121.08 (16)
C5—C6—C7	119.87 (18)	C13—C14—C9	123.19 (15)
C5—C6—H6	120.1	C13—C14—H14	118.4
C7—C6—H6	120.1	C9—C14—H14	118.4
C6—C7—C2	118.54 (14)	C13—C15—H15A	109.5
C6—C7—N2	124.92 (15)	C13—C15—H15B	109.5
C2—C7—N2	116.51 (14)	H15A—C15—H15B	109.5
N2—C8—C9	122.03 (13)	C13—C15—H15C	109.5
N2—C8—H8	119.0	H15A—C15—H15C	109.5
C9—C8—H8	119.0	H15B—C15—H15C	109.5
C14—C9—C10	117.90 (14)	C10—O1—H1	109.5
C14—C9—C8	120.05 (13)	C8—N2—C7	121.58 (13)
C7—C2—C3—C4	-0.4 (3)	C14—C9—C10—C11	-1.4 (2)
C1—C2—C3—C4	179.34 (17)	C8—C9—C10—C11	179.69 (14)
C2—C3—C4—C5	1.2 (3)	O1—C10—C11—C12	-179.53 (15)
C3—C4—C5—C6	-0.4 (3)	C9—C10—C11—C12	0.8 (2)
C4—C5—C6—C7	-1.1 (3)	C10—C11—C12—C13	0.4 (3)
C5—C6—C7—C2	1.9 (2)	C11—C12—C13—C14	-0.9 (3)
C5—C6—C7—N2	179.77 (15)	C11—C12—C13—C15	179.52 (18)
C3—C2—C7—C6	-1.1 (2)	C12—C13—C14—C9	0.3 (2)
C1—C2—C7—C6	179.13 (15)	C15—C13—C14—C9	179.81 (17)
C3—C2—C7—N2	-179.21 (14)	C10—C9—C14—C13	0.9 (2)
C1—C2—C7—N2	1.1 (2)	C8—C9—C14—C13	179.80 (14)
N2—C8—C9—C14	-178.55 (13)	C9—C8—N2—C7	-178.75 (13)
N2—C8—C9—C10	0.3 (2)	C6—C7—N2—C8	25.3 (2)
C14—C9—C10—O1	178.93 (14)	C2—C7—N2—C8	-156.72 (13)
C8—C9—C10—O1	0.0 (2)		

Hydrogen-bond geometry (Å, °)

Cg1 is the centroid of the C9—C14 ring.

D—H···A	D—H	H···A	D···A	D—H···A
O1—H1···N2	0.92	1.83	2.6280 (16)	145
C4—H4···N1 ⁱ	0.93	2.77	3.610 (3)	150
C15—H15A···O1 ⁱⁱ	0.96	2.74	3.641 (3)	158
C11—H11···Cg1 ⁱⁱⁱ	0.93	2.85	3.654 (16)	146

Symmetry codes: (i) $-x+1/2, -y+1, z+1/2$; (ii) $x, -y+1/2, z+1/2$; (iii) $x+1/2, -y+1/2, -z+1$.